

Very Large Array (VLA) Measurements of Coronal Angular Broadening

Jason E. Kooi¹, Avni Singh², Prateek Bardhan³, & Ian Sutcliffe⁴

1. Measuring Coronal B

Understanding the strength and structure of the coronal magnetic field is critical because it is the dominant energy source for producing the solar wind and energetic solar activity. Faraday rotation is one of the few diagnostic tools with which to probe **B** and **B** fluctuations of the corona.

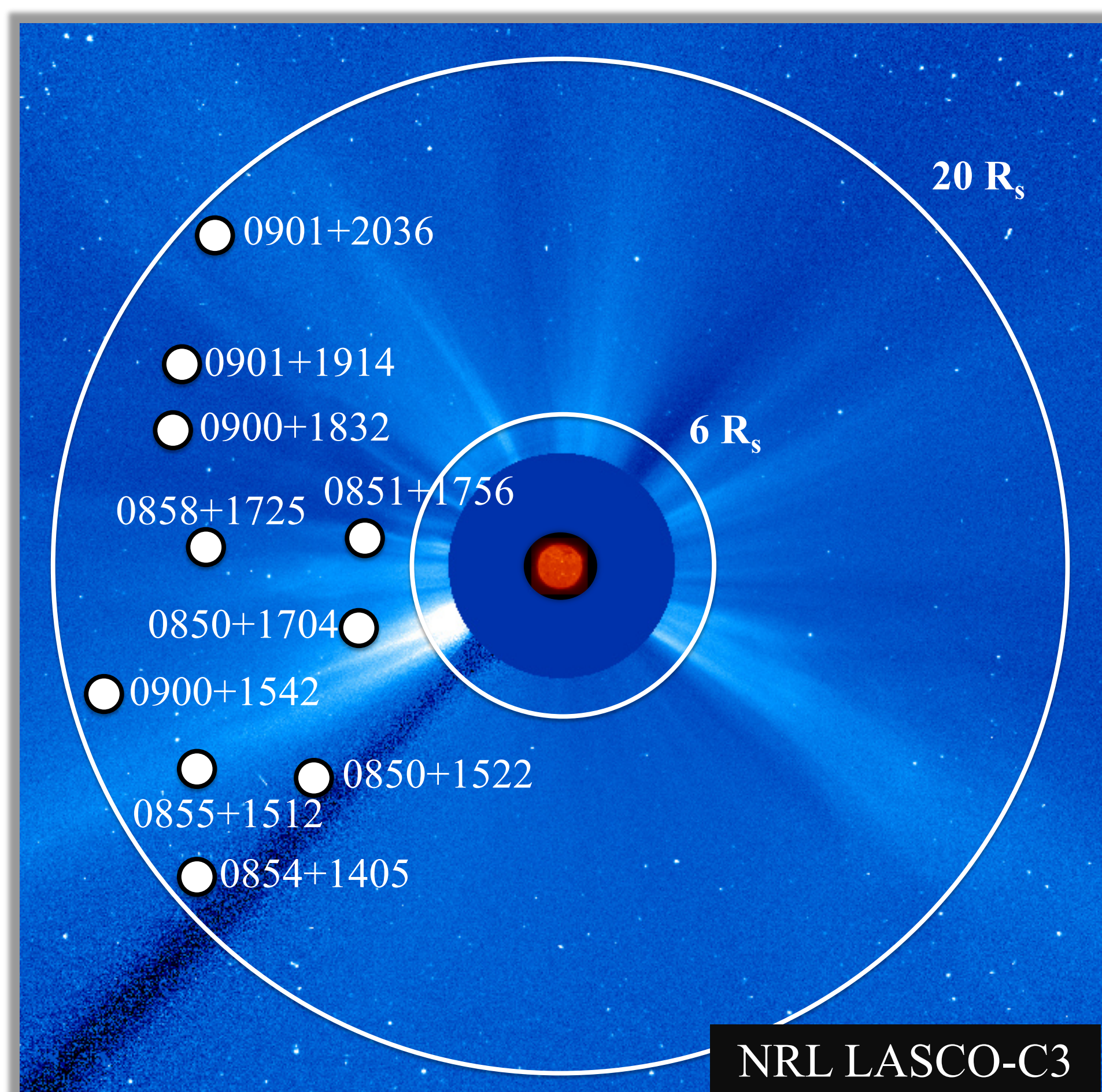


Fig. 1 – Solar corona on July 31, 2015, as observed with the LASCO-C3 coronagraph and SDO AIA 304. The white plotted points are the lines of sight (LOS) to radio sources (identified by J2000 RA & DEC coordinates) at 20:06 UT.

2. Faraday Rotation (FR)

Faraday rotation is the change in the polarization position angle of polarized radiation as it propagates through a magnetized plasma (with density n_e). In cgs, $\Delta\chi$ is given by

$$\Delta\chi = \chi - \chi_0 \equiv \left[C_{FR} \int_{LOS} n_e B_{LOS} ds \right] \lambda^2 = [RM] \lambda^2 \quad \text{Eq. 1}$$

Here, $C_{FR} = 2.631 \times 10^{-17} \text{ rad-G}^{-1}$, B_{LOS} is the magnetic field component along the line of sight in the direction of the observer, and λ is the observational wavelength.

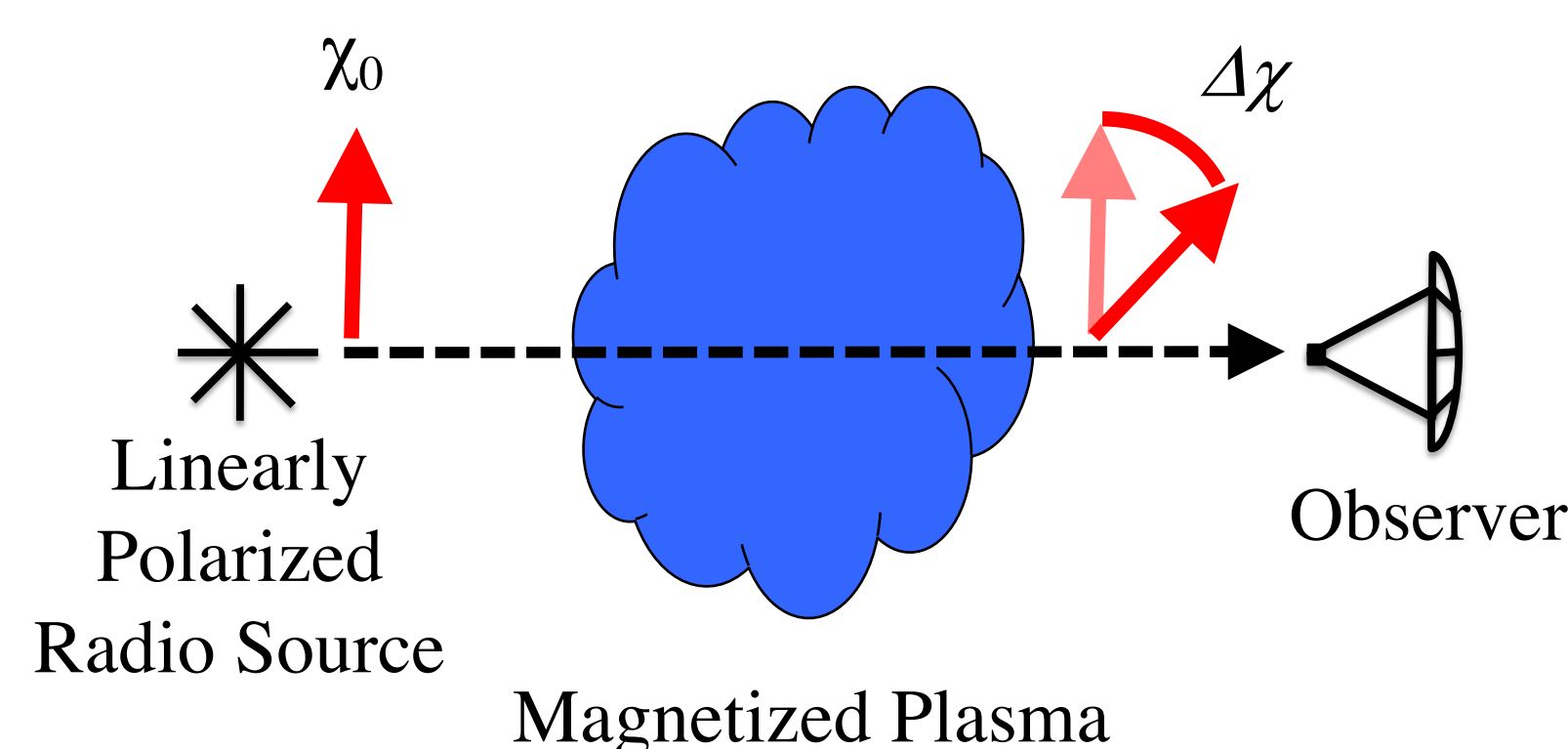


Fig. 2 – Illustration of the LOS from a radio source, through a magnetized plasma (e.g., CME), to a radio telescope on Earth.

3. Observe Background Radio Sources Using the VLA

We made full-polarization observations at 1 – 2 GHz frequencies using the Karl G. Jansky Very Large Array of 21 linearly polarized cosmic radio sources occulted by the solar corona in July and August, 2015. Observations were made in A array configuration and so the longest baselines are ~ 37 km. A typical radio map is demonstrated below.

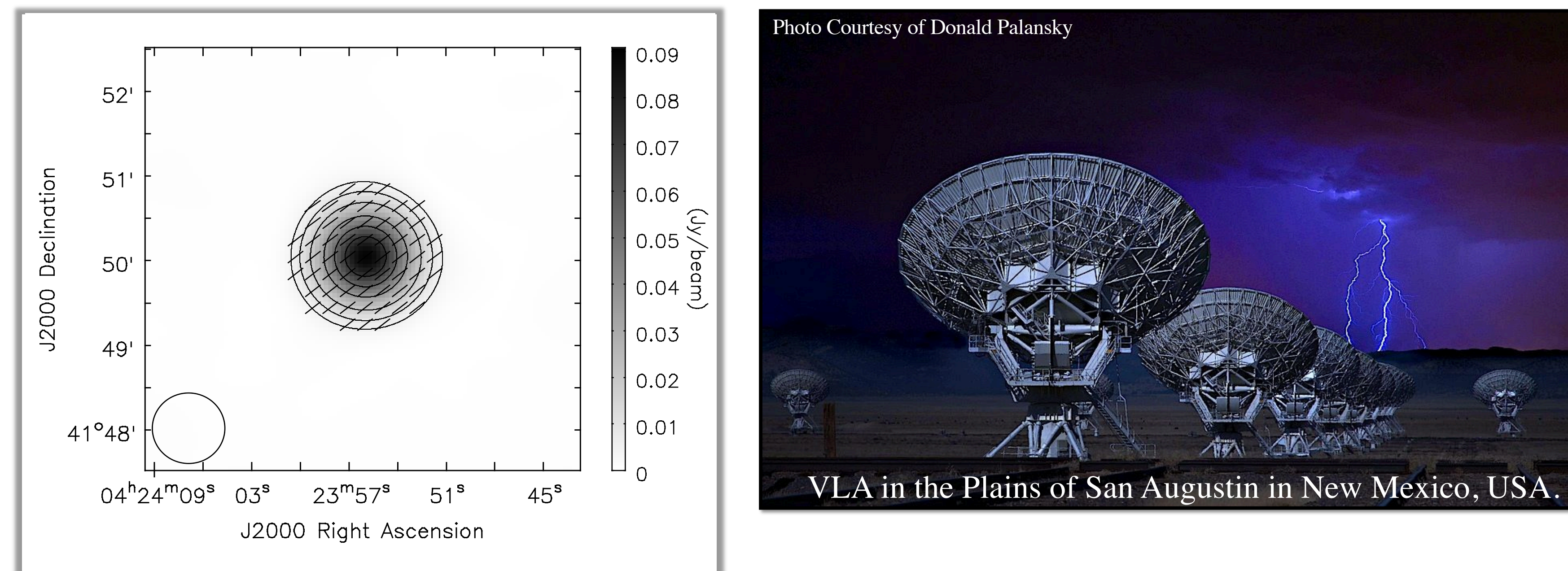


Fig. 3 – Radio map of the polarization structure of 4C 41.11. Image is a synthesis of the 48 MHz bandpass centered at a frequency of 1.365 GHz. The contours show the distribution of total intensity, I , and are plotted at 5, 10, 20, 40, 60, and 80% of the peak intensity (1.543 Jy/beam). The grayscale indicates the magnitude of linearly polarized intensity, P . The orientation of the line segments gives polarization position angle χ . The synthesized beam (resolution) is plotted in the lower left corner of the figure.

5. Coronal Angular Broadening in Radio Maps

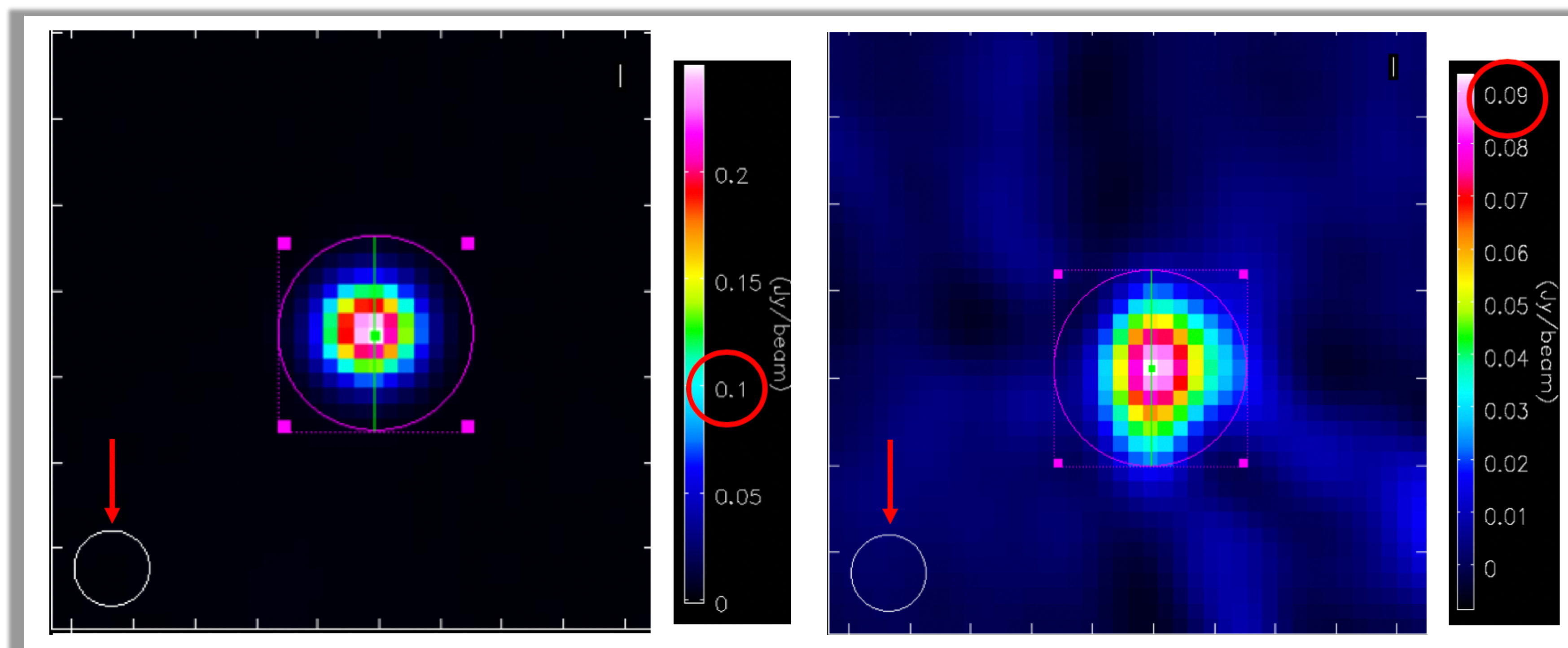


Fig. 4 – Radio maps of the total intensity (in Jy/beam) of the radio source 0839+1802 on a reference day (left – no angular broadening present) and on the day of occultation by the corona (right – angular broadening present). The resolution of the image (FWHM diameter of the synthesized beam) is 1.75 arcsec. The red arrows highlight the synthesized beam in the lower left corner of the each figure. The green vertical line and pink circle and square outline the region analyzed to determine the impact of the angular broadening. The red circles on the total intensity scales demonstrate the reduction in intensity from the reference observations to the occultation observations.

4. Angular Broadening

Angular broadening results from plasma density irregularities elongated along the coronal magnetic field that cause radio wave scattering.

- Measured intensity (Stokes I in Figures 3 and 4) is the convolution of the true radio source intensity with a point spread function (PSF, the effective response of an imaging system to an unresolved, point-like source).
- In most applications, the PSF is simply the synthesized beam; however, when observing through a turbulent plasma like the corona, the PSF is the convolution of the synthesized beam with the power pattern of the angular broadening.
- Angular broadening acts to reduce the measured intensity of a radio source (Eq. 2).**
- This can have important consequences for coronal Faraday rotation studies because the error associated with measuring the polarization angle, χ , is inversely proportional to the intensity of the linearly polarized light.

$$\frac{I_{occ}}{I_{ref}} = \frac{\theta_{major} * \theta_{minor} (ref)}{\theta_{major} * \theta_{minor} (Occ)} \quad \text{Eq. 2}$$

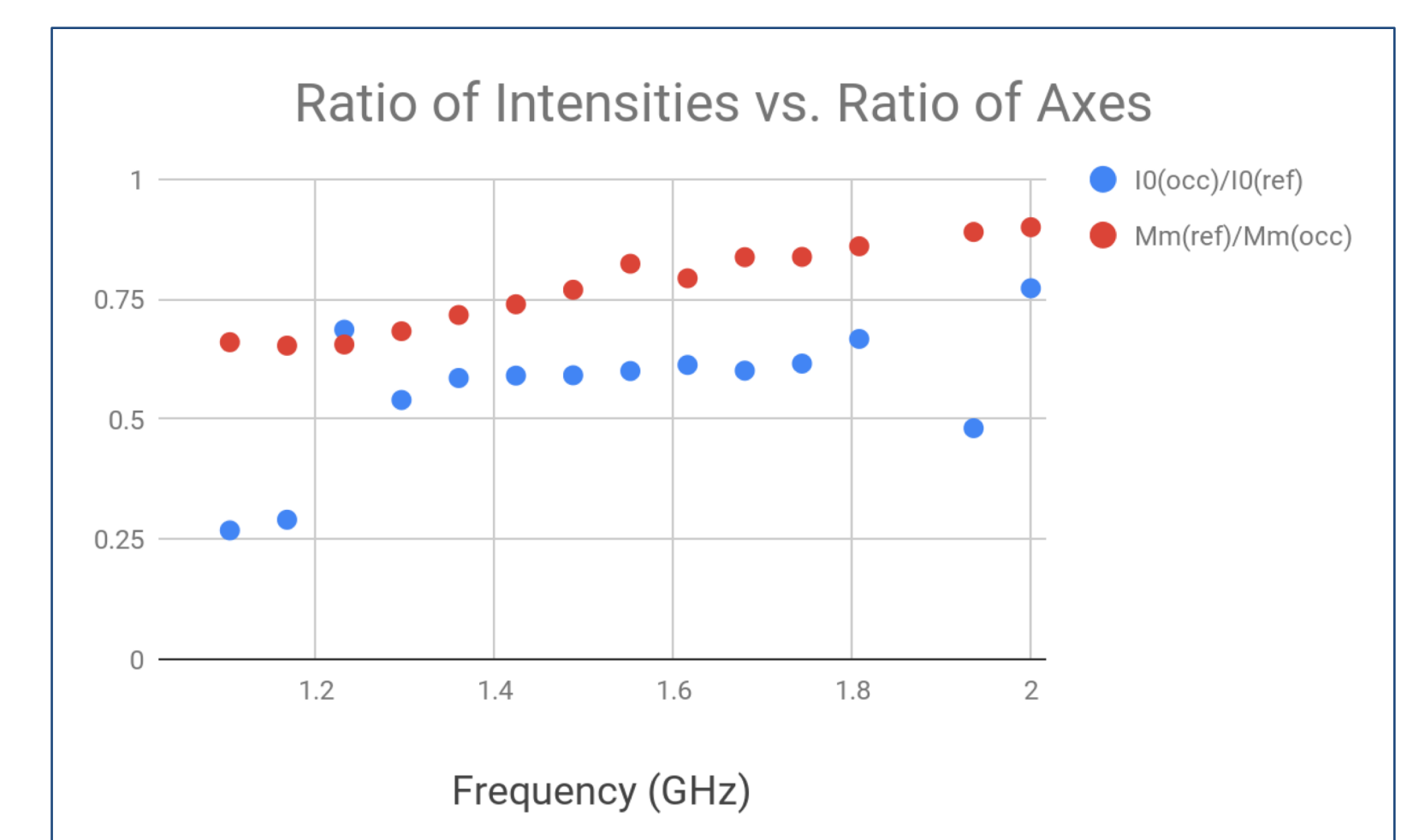
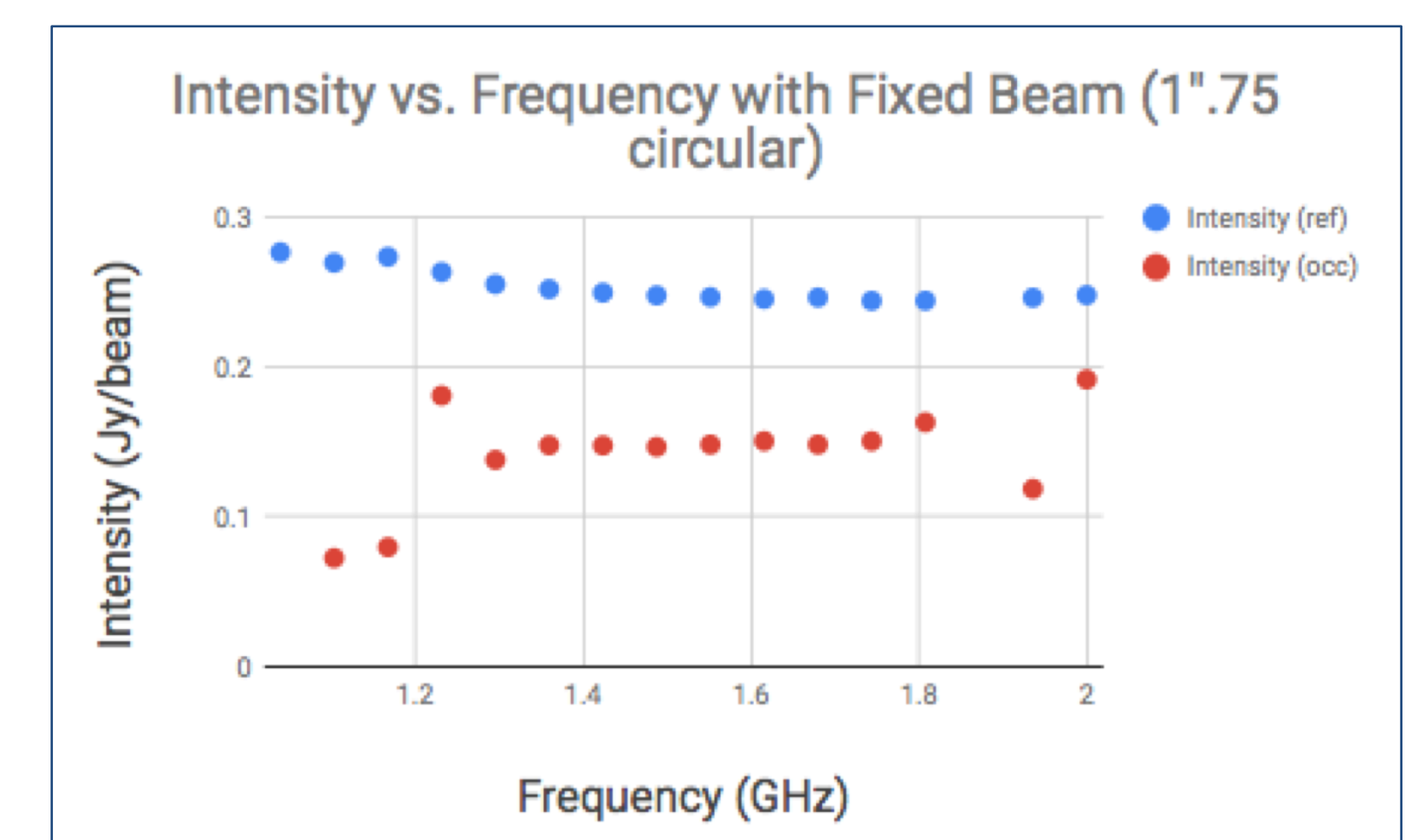


Fig. 5 – Top: Total Intensity vs. frequency of observation. Blue data are measurements from a reference day (ref) and red data are measurements made when the source was occulted (occ) by the corona. The significant reduction in total intensity at low frequencies is a result of noisier radio maps. Bottom: comparison of the ratio of intensities (blue, LHS of Eq. 2) and the ratio of the source structure (red, RHS of Eq. 2).

1. U.S. Naval Research Laboratory, Code 7213, 4555 Overlook Ave. SW, Washington, DC 20375, USA
2. Volgenau School of Engineering, George Mason University, 4400 University Drive, Fairfax, VA 22030, USA
3. Department of Astronomy, University of Texas at Austin, 2515 Speedway, Stop C1400, Austin, TX 78712, USA
4. Computer Science Department, University of Virginia, Thornton Hall, P.O. Box 400259, Charlottesville, VA 22904, USA

This work was supported at the U.S. Naval Research Laboratory by the Jerome and Isabella Karle Distinguished Scholar Fellowship program and by the Science and Engineering Apprenticeship Program (SEAP).